Progress In Electromagnetics Research, Vol. 145, 93–113, 2014

A Rapid Accurate Technique to Calculate the Group Delay, Dispersion and Dispersion Slope of Arbitrary Radial Refractive Index Profile Weakly-Guiding Optical Fibers

Raushan Mussina[1, *], David R. Selviah[1], F. Aníbal Fernández[1], Anton G. Tijhuis[2], and Bastiaan P. de Hon[2]

Abstract—This paper introduces a new numerical method to calculate the group delay, chromatic dispersion and dispersion slope of weakly-guiding optical fibers with arbitrary radial refractive index profiles. It is based on the analytical differentiation of the propagation coefficient up to the third order. The simulation results are compared to experimental data, with those calculated by other approaches and exact data where possible. Due to the analytical differentiation of the matrix equation, the method is more accurate compared to other approaches, it is also much faster than numerical differentiation as allows avoiding repeated solution of the eigenvalue problem to calculate the derivatives of the propagation coefficient. The precision of the method is limited only by the approximation errors of the mode solver. The Galerkin method with Laguerre-Gauss basis functions is used to determine the propagation coefficients of weakly-guiding structures. The new method enables fiber manufacturers to rapidly design dispersion characteristics of graded index, step index, single- and multiple-clad fibers, as well as few-mode and bend insensitive fibers.

1. INTRODUCTION

In order to meet the increasing demand for higher transmission bandwidths through single mode optical fibers, using higher bit rates and/or an increased number of wavelength channels, more attention is being paid to suitably tailoring the optical fiber's chromatic dispersion characteristics. Accurate and fast numerical modeling methods are required to design the optimum refractive index profiles for single mode fibers to give specific dispersion characteristics. Modeling enables many refractive index profiles to be investigated and optimized without the need for costly and time consuming experimental fabrication and measurements. Over the past decades, numerous approximate techniques have been developed for the calculation of the dispersion parameters for single-mode optical fibers [1–11] and a variety of refractive index profiles were designed and analyzed to achieve the desired dispersion characteristics [12–23].

The dispersion characteristics of an optical fiber, namely the group delay, τ_g, dispersion, D, and the dispersion slope, DS, are proportional to the first, second and third-order derivatives of the propagation coefficient, β, with respect to wavelength respectively. Therefore, it is first necessary to calculate an accurate approximation of the propagation coefficient, by solving the scalar wave equation (assuming a weakly guiding optical fiber model), as the accuracy of this approximation determines the accuracy of the derivatives calculated from it. It has been shown that even giving sufficient approximation of the propagation coefficient, some techniques are not accurate enough to obtain its derivatives [1].

Received 12 March 2013, Accepted 11 October 2013, Scheduled 1 March 2014

* Corresponding author: Raushan Mussina (r.mussina@ee.ucl.ac.uk).

[1] Department of Electronic and Electrical Engineering, University College London, UCL, London, WC1E 7JE, UK. [2] Faculty of Electrical Engineering, University of Technology, 5600 MB Eindhoven, The Netherlands.

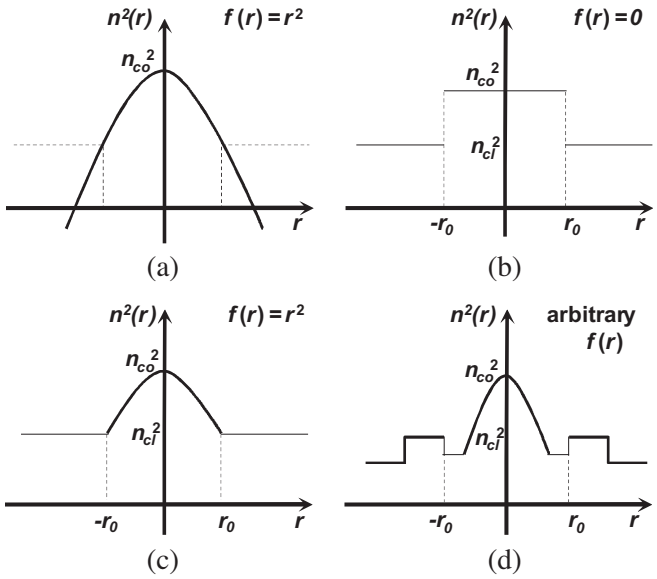

Figure 1. Schematic refractive index profiles: (a) infinitely extended parabolic profile; (b) step-index profile; (c) truncated parabolic profile; (d) arbitrary profile.

One of the most powerful, accurate, yet simple techniques to find the solution of the scalar wave equation is the Galerkin method which in this case coincides with the Rayleigh-Ritz variational method [24]. The Galerkin method [25–34] has been used to calculate the propagation coefficients and modal fields of optical fibers and rectangular and slab dielectric-waveguides, with the aid of different sets of entire basis functions such as Bessel functions, Laguerre-Gauss or Hermite-Gauss polynomial functions. These have the advantages that: a) they form complete sets of orthonormal functions which satisfy the boundary conditions (the fields are finite at the waveguide axis and decay to zero at an infinite lateral distance from the axis), b) they represent the solutions of a problem with a similar geometry: Bessel functions are the eigensolutions of the scalar wave equations for step-index circular core fibers while Laguerre-Gauss and Hermite-Gauss polynomials are the eigenmodes of an infinitely extended parabolic refractive index profile in circular and rectangular waveguide geometries respectively (see Figure 1(a)). In addition, the coupling loss between two spliced or connected optical fibers can be easily found by expressing the power transmission coefficients in the form of a weighted sum of simple generalized Laguerre polynomials so that the time consuming and approximate numerical calculation of overlap integrals is avoided [35].

The Galerkin method has also been used as the mode solver for the dispersion analysis of single-mode optical fibers [2, 3]. For dispersion analysis, in [3] Bessel functions were used as the basis functions and dispersion was calculated by numerical differentiation of the propagation coefficient. Sharma and Banerjee [2] employed Laguerre-Gauss polynomials as the basis functions and proposed an approach based on matrix perturbation theory for the calculation of the first and second derivatives of the propagation coefficient. Numerical differentiation of the propagation coefficient was also used in [4]. Two further approaches for the determination of the dispersion coefficient based on an equivalent transmission-line technique and a variational finite-element formulation were considered in [5, 6].

If the optical fields are expanded in terms of entire functions such as Laguerre-Gauss polynomials then further analytical work can be carried out based on the results. In this paper, we propose an analytical method for the calculation of the derivatives of the propagation coefficient by directly differentiating the matrix equation resulting from the Galerkin method with Laguerre-Gauss basis functions. The symmetric system of linear equations in the eigenvalue problem is ideally suited to repeated differentiation giving the opportunity to calculate not only the group delay and dispersion, but also the dispersion slope. An analytical approach for the evaluation of the first and second derivatives of the propagation coefficient for photonic crystal fibers was recently reported in [36] where the time required for the calculation of a single dispersion value at a fixed wavelength was about 5 min. To

our knowledge, research to date has tended to focus on methods to calculate dispersion and have not included the calculation of dispersion slope. However, for the design of optical fibers knowledge of the dispersion slope is now becoming as important as the knowledge of the dispersion coefficient. In addition, the speed of the calculation technique is quite important if the technique is embedded in an optimization procedure when the fiber characteristics are calculated thousands or hundreds of thousands times. When numerical differentiation (first and higher order finite differences method) is used for the calculation of the propagation coefficient derivatives, then, in addition to introducing approximation errors, the overall method becomes rather slow as in this case the eigenvalue problem is usually solved five times for the determination of dispersion and dispersion slope.

In the proposed method, the computation of the second and third derivatives of the propagation coefficient involves the determination of the first and second derivatives of the eigenvectors for which the eigenvalue problem is solved two more times. Thus, in the present approach, the eigenvalue problem is solved in all only three times while giving the derivatives free of errors related to approximate differentiation. The idea is to combine a very fast and effective mode solver of the scalar wave equation with exact differentiation to achieve better accuracy and obtain an effective method for the calculation of dispersion characteristics. Although the initial analytical differentiation of the matrix elements is cumbersome this only needs to be done once and the details are provided explicitly in this paper. After it has been programmed, the approach gives a fast technique for calculation of the dispersion characteristics of single-mode optical fibers. This paper demonstrates such a computer program employed for analyzing the dispersion of single-mode optical fibers with radially arbitrary refractive index profiles. The wavelength dependence of the refractive indices of the core and cladding materials are incorporated in the model so that the program calculates the total chromatic dispersion; the program can also calculate the dispersion properties of the waveguide alone when the material wavelength dependence is ignored.

The paper is laid out as follows: Section 2 provides the theoretical principles underlying the technique by first giving a brief review of fiber dispersion parameters and describes the proposed method for their calculation. Section 3 presents the simulation results and discusses the validity of the approach and compares the simulation results to available exact, experimental and published data. The paper concludes in Section 4. The paper also contains two appendices with differentiation details of the matrix elements and the short description of the Galerkin method applied to optical fiber model to aid the reader.

2. MODELING METHOD MATHEMATICAL FUNDAMENTALS

2.1. Optical Fiber Dispersion Parameters: Group Delay, Dispersion, and Dispersion Slope

The wavelength or frequency-dependent nature of dispersion is described by the group delay time, τ_g, per unit length. This group slowness is the reciprocal of the group velocity, υ_g, at which a pulse propagates through the fiber [37]:

$$\tau_g \triangleq \frac{1}{\upsilon_g} \triangleq \frac{d\beta}{d\omega}. \tag{1}$$

The dispersion, D, per unit length is defined as [37]

$$D \triangleq \frac{d\tau_g}{d\lambda} = -\frac{\lambda}{c}\frac{d^2}{d\lambda^2}\left(\frac{\beta}{k_0}\right) = -\frac{2\pi c}{\lambda^2}\frac{d^2\beta}{d\omega^2}, \tag{2}$$

where c is the speed of light in a vacuum. This formula can also be used for the calculation of material dispersion, D_m, if β/k_0 is replaced by the material refractive index $n(\lambda)$ [13]:

$$D_m = -\frac{\lambda}{c}\frac{d^2 n\left(\lambda\right)}{d\lambda^2}. \tag{3}$$

One often defines the single-mode waveguide dispersion, D_w, as the dispersion obtained from the scalar wave equation by neglecting the wavelength-dependence of the refractive indices of the materials

of the fiber. Subsequently, the total dispersion D is then approximated as the sum of the material dispersion, D_m, and waveguide dispersion, D_w, i.e.,

$$D \approx D_m + D_w. \tag{4}$$

This paper proposes that the total dispersion, D, be calculated instead by using Equation (2). Subsection 3.4 compares the result of calculating the total dispersion, D, using Equation (2) with the result calculated using the approximation $D_m + D_w$ in Equation (4) for a variety of single mode fibers of different designs.

For wavelength division multiplexing, WDM, the next (third) order derivative becomes important. It is called *the dispersion slope* which is the derivative of the dispersion, D, with respect to wavelength [13]:

$$DS = \frac{dD}{d\lambda}. \tag{5}$$

In the presence of only the dispersion slope, a pulse suffers asymmetric distortion [13].

2.2. The Proposed Method: Calculation of Single-Mode Fiber Dispersion Characteristics

The application of the Galerkin method to a weakly-guiding optical fiber model is described in full detail in [25] by Meunier et al. Here we recall that the method results in a matrix eigenvalue problem

$$\mathbf{A}\mathbf{c} = \beta^2\mathbf{c}, \tag{6}$$

where $\mathbf{A}$ is a real symmetric matrix, β the propagation coefficient, and the components of the eigenvectors $\mathbf{c}$ represent the mode field expansion coefficients in terms of basis functions.

Below, the proposed algorithm for the calculation of dispersion characteristics of single-mode fibers is presented. As shown in Subsection 2.1, the first, second and third order derivatives of the propagation coefficient with respect to wavelength (or frequency) are needed to calculate the group delay, τ_g, dispersion, D, and the dispersion slope, DS. To obtain these derivatives we directly differentiate matrix Equation (6) and the condition for the normality of the eigenvector

$$\|\mathbf{c}\| = 1 \quad \text{or} \quad \mathbf{c}^T\mathbf{c} = 1, \tag{7}$$

with respect to frequency, ω; here $\mathbf{c}^T$ is the transpose of $\mathbf{c}$.

All of the terms in Equation (6) $\mathbf{A}$, β^2 and $\mathbf{c}$ depend on the angular frequency, ω. So, differentiation of Equations (6) and (7) with respect to ω gives

$$\frac{d\mathbf{A}}{d\omega}\mathbf{c} + \mathbf{A}\frac{d\mathbf{c}}{d\omega} = \frac{d\beta^2}{d\omega}\mathbf{c} + \beta^2\frac{d\mathbf{c}}{d\omega}, \tag{8}$$

and

$$\frac{d\mathbf{c}^T}{d\omega}\mathbf{c} + \mathbf{c}^T\frac{d\mathbf{c}}{d\omega} = 0 \;\Rightarrow\; \mathbf{c}^T\frac{d\mathbf{c}}{d\omega} = 0. \tag{9}$$

Multiplication of (8) by $\mathbf{c}^T$ on the left results in

$$\mathbf{c}^T\frac{d\mathbf{A}}{d\omega}\mathbf{c} + \mathbf{c}^T\left(\mathbf{A} - \beta^2\mathbf{I}\right)\frac{d\mathbf{c}}{d\omega} = \frac{d\beta^2}{d\omega}\mathbf{c}^T\mathbf{c}, \tag{10}$$

which, due to (7) and $\mathbf{c}^T(\mathbf{A} - \beta^2\mathbf{I}) = 0$ (this is due to the symmetry of $\mathbf{A}$), gives

$$\frac{d\beta^2}{d\omega} = \mathbf{c}^T\frac{d\mathbf{A}}{d\omega}\mathbf{c}, \tag{11}$$

or equivalently,

$$\frac{d\beta}{d\omega} = \frac{1}{2\beta}\mathbf{c}^T\frac{d\mathbf{A}}{d\omega}\mathbf{c}. \tag{12}$$

This is the first derivative of the propagation coefficient. To calculate it we need to find $d\mathbf{A}/d\omega$, the derivative of matrix $\mathbf{A}$, which we do by differentiating the terms of $\mathbf{A}$ analytically.

Similarly, by differentiating now Equation (8), we have

$$\frac{d^2\mathbf{A}}{d\omega^2}\mathbf{c}+2\frac{d\mathbf{A}}{d\omega}\frac{d\mathbf{c}}{d\omega}+\mathbf{A}\frac{d^2\mathbf{c}}{d\omega^2}=\frac{d^2\beta^2}{d\omega^2}\mathbf{c}+2\frac{d\beta^2}{d\omega}\frac{d\mathbf{c}}{d\omega}+\beta^2\frac{d^2\mathbf{c}}{d\omega^2}. \tag{13}$$

Multiplying the last equation by $\mathbf{c}^T$ on the left and taking into account Equations (7) and (9) and that $\mathbf{c}^T\left(\mathbf{A}-\beta^2\mathbf{I}\right)=0$, we derive

$$\frac{d^2\beta^2}{d\omega^2}=\mathbf{c}^T\left(\frac{d^2\mathbf{A}}{d\omega^2}\right)\mathbf{c}+2\mathbf{c}^T\frac{d\mathbf{A}}{d\omega}\frac{d\mathbf{c}}{d\omega}. \tag{14}$$

Then the last expression is used to calculate the second derivative of the propagation coefficient

$$\frac{d^2\beta}{d\omega^2}=\frac{1}{2\beta}\left[\frac{d^2\beta^2}{d\omega^2}-2\left(\frac{d\beta}{d\omega}\right)^2\right]. \tag{15}$$

Finally, we differentiate now Equation (13)

$$\frac{d^3\mathbf{A}}{d\omega^3}\mathbf{c}+3\frac{d^2\mathbf{A}}{d\omega^2}\frac{d\mathbf{c}}{d\omega}+3\frac{d\mathbf{A}}{d\omega}\frac{d^2\mathbf{c}}{d\omega^2}+\mathbf{A}\frac{d^3\mathbf{c}}{d\omega^3}=\frac{d^3\beta^2}{d\omega^3}\mathbf{c}+3\frac{d^2\beta^2}{d\omega^2}\frac{d\mathbf{c}}{d\omega}+3\frac{d\beta^2}{d\omega}\frac{d^2\mathbf{c}}{d\omega^2}+\beta^2\frac{d^3\mathbf{c}}{d\omega^3}. \tag{16}$$

Again, multiplying this by $\mathbf{c}^T$ on the left and taking into account Equations (7) and (9) and that $\mathbf{c}^T\left(\mathbf{A}-\beta^2\mathbf{I}\right)=0$, we get

$$\frac{d^3\beta^2}{d\omega^3}=\mathbf{c}^T\left(\frac{d^3\mathbf{A}}{d\omega^3}\right)\mathbf{c}+3\mathbf{c}^T\left(\frac{d^2\mathbf{A}}{d\omega^2}\right)\frac{d\mathbf{c}}{d\omega}+3\mathbf{c}^T\left(\frac{d\mathbf{A}}{d\omega}-\frac{d\beta^2}{d\omega}\mathbf{I}\right)\frac{d^2\mathbf{c}}{d\omega^2}. \tag{17}$$

And the third derivative of β is calculated by

$$\frac{d^3\beta}{d\omega^3}=\frac{1}{2\beta}\left[\frac{d^3\beta^2}{d\omega^3}-6\frac{d\beta}{d\omega}\frac{d^2\beta}{d\omega^2}\right]. \tag{18}$$

Equations (15) and (18) are derived by repeated differentiation (with respect to frequency) of

$$\frac{d\beta^2}{d\omega}=2\beta\frac{d\beta}{d\omega}. \tag{19}$$

From Equations (14) and (17) it can be seen that the second and third derivatives of β require the first, second and third derivatives of $\mathbf{A}$ and the first and second derivatives of the eigenvector $\mathbf{c}$. There are various techniques designed to calculate eigenvector derivatives of real symmetric eigensystems, two of such methods are described, for example, in [38, 39]. The second and third derivatives of matrix $\mathbf{A}$ are defined by repeatedly differentiating the terms of matrix $\mathbf{A}$. This is described in the next Subsection, 2.3, and in Appendix A "The derivatives of the matrix elements".

2.3. Derivatives of the Matrix A

Appendix B provides the short description of the theory developed by Meunier et al. [25] that applies the Galerkin method to optical fiber model and shows how the symmetric matrix $\mathbf{A}$ in Equation (6) is obtained. The matrix has terms

$$\begin{aligned} a_{ij} &= k_0^2\left\langle b_i^m, \left(n^2(r)-n_0^2(r)\right)b_j^m\right\rangle+\beta_0^2\delta_{i,j} \\ &= K^m_{(i-1)(j-1)}\left(I^m_{(i-1)(j-1)}+J^m_{(i-1)(j-1)}\right)+\beta_0^2\delta_{i,j} \end{aligned} \tag{20}$$

where k_0 is the free-space wavenumber, $b_i^m(x(r))$ are the Laguerre-Gauss basis functions, m is the azimuthal mode number, δ_{ij} is the Kronecker delta, and

$$K_{ij}^m = 2\Delta k_0^2 n_{co}^2\left[\frac{(i+m)!}{i!}\frac{(j+m)!}{j!}\right]^{-1/2} \tag{21}$$

$$I_{ij}^m = \int_0^V e^{-x}x^m L_i^m(x)\left\{1-f\left(\sqrt{x/V}\right)\right\}L_j^m(x)\,dx \tag{22}$$

$$J_{ij}^m = \int_0^\infty e^{-x}x^m L_i^m(x)\left[x/V-1\right]L_j^m(x)\,dx \tag{23}$$

the relative refractive index $\Delta = (n_{co}^2 - n_{cl}^2)/\left(2n_{co}^2\right)$, V is the normalized frequency defined as $V = k_0 r_0 \sqrt{n_{co}^2 - n_{cl}^2}$, n_{co} and n_{cl} are the refractive indices at the core center and the cladding of the fiber, respectively, x is the normalized radial coordinate $x(r) = V(r/r_0)^2$, r_0 is the core radius, $L_i^m(x)$ are generalized Laguerre polynomials, and $n(r)$ is the refractive index profile of the fiber which is expressed by:

$$n^2(r) = \begin{cases} n_{co}^2 \left[1 - 2\Delta f\left(r/r_0\right)\right], & r \le r_0 \\ n_{cl}^2 = n_{co}^2 \left[1 - 2\Delta f\left(1\right)\right], & r > r_0 \end{cases} \tag{24}$$

where the profile function $f(r/r_0)$ is normalized so that $f(0) = 0$ and $f(1) = 1$; the first three derivatives of $f(r/r_0)$ with respect to its argument, r/r_0, are used when the matrix equation in (6) is repeatedly differentiated with respect to ω (this is because in Equation (22) the argument of function f is frequency dependent). Figure 1(a) shows the reference infinitely extended parabolic profile, $n_0(r)$, for which the Laguerre-Gauss polynomials are the eigenmodes with the propagation coefficients, $\beta_0^2 = k_0^2 n_{co}^2 \left[1 - 2\Delta \frac{2i+m+1}{V/2}\right]$. The schematic refractive index profiles are given in Figures 1(b), (c) and (d): (b) step-index, (c) truncated parabolic (or graded) and (d) more complicated refractive index profiles. The combination of step and graded refractive index profiles, such as in Figure 1(d), is considered in [12] for the design of dispersion compensating fibers. The Sellmeier equations, Equation (A9), are used to take into account the wavelength dependence of the refractive indices of the core and cladding materials [40].

The expressions for K_{ij}^m and β_0^2 are easy to differentiate, although all the constituents k_0, Δ, V and n_{co}^2 in these expressions are frequency-dependent. The integrals J_{ij}^m can be expressed analytically [25] where only V is frequency-dependent, and are also easy to differentiate.

In I_{ij}^m, both V and x depend on frequency. The Leibniz integral rule for integrals with variable limits [41] is used for taking the derivatives of I_{ij}^m and this process is rather laborious, especially in the case of the third-order derivatives.

To aid the reader the expressions for the derivatives of the matrix elements resulting from this process are provided in Appendix B "The derivatives of the matrix elements".

3. NUMERICAL RESULTS

A computer program that utilizes the proposed approach was developed to calculate the propagation coefficients, the electric field distributions and the dispersion characteristics of weakly-guiding optical fibers with arbitrary radial refractive-index profiles. Simulations for a range of different refractive index profiles were carried out to test the accuracy and validity of the method. Several examples that have been considered previously in [2, 3, 6, 7, 16, 18] were used for validation. The analysis of the convergence of the proposed method and comparison of its accuracy with that of other methods is given in Subsection 3.2. Subsection 3.3 provides the comparison of the simulation results to the exact data available only for step-index fibers. In the next Subsection, 3.1, our simulated dispersion graphs are plotted. We do not provide comparative graphs as they are visually indistinguishable from those in the above-mentioned research papers. We present here our own graphs except for the example considered in Subsection 3.1 b) where our simulated dispersion is compared to available experimental data from [7].

3.1. Dispersion Graphs

a) The first example is a dispersion-shifted step-index fiber with zero total dispersion at 1.55 μm wavelength and a non-zero dispersion shifted fiber with a triangular profile considered in [2]. Both fibers have pure silica cladding and a 13.5% germania-doped silica core. In Figure 2(a) the dispersion is plotted against wavelength for both fibers and the graphs are identical to those shown in Figure 1 of [2].

b) Next is an example that compares simulation results with experimental data given in [7] for a depressed cladding fiber with a 3.9% Ge-doped plasma induced chemical vapor deposition (PCVD) silica core region surrounded by a 1% fluorine-doped PCVD silica region that forms the depressed cladding

and pure silica outer cladding (the radii are 3.5 and 30 µm). The Sellmeier parameters for germania and fluorine doped PCVD silica are defined according to expressions given in [7]. A good agreement was established between the simulated and experimental data as can be seen from Figure 2(b).

c) A triple-clad fiber with an undoped silica core and F-doped claddings that has two zeros of chromatic dispersion occurring at 1.30 µm and 1.55 µm was designed in [16]. The refractive index profile of the fiber is depicted in Figure 3(b) with the following parameters: $\Delta_1 = 0.63\%$, $\Delta_2 = 0.18\%$ and $\Delta_3 = 0.40\%$ and the radii R_1, R_2 and R_3 equal 4.2 µm, 8.25 µm and 15.0 µm, respectively. The chromatic dispersion of the fiber is represented in Figure 3(a) by the light green curve.

The dispersion curve, in fact, has three zeros and their sensitivity to the drawing ratio, defined as the ratio of preform diameter to fiber diameter, was analyzed in [16]. For this a radial scale factor, F, was introduced so that increasing F means proportionally increasing the cladding radii R_1, R_2 and R_3. The dispersion values were recalculated for slightly changing F from 0.97 to 1.03 using the proposed

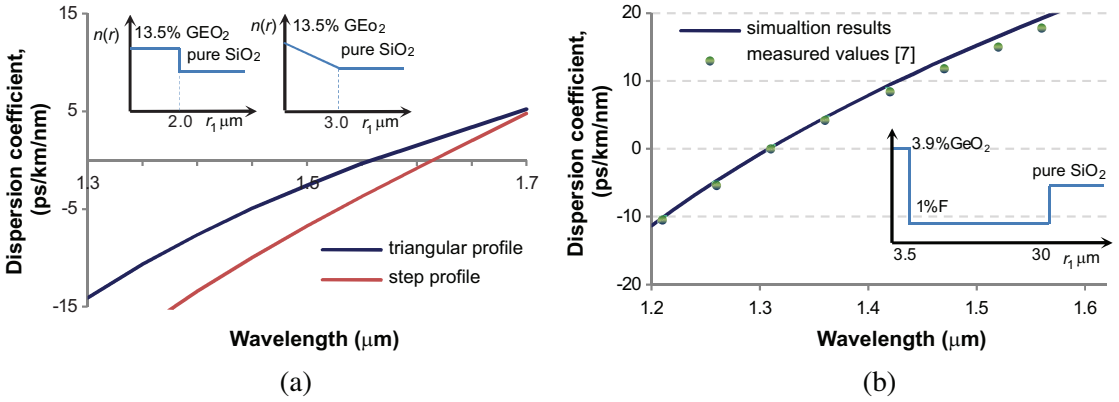

(a) (b)

Figure 2. Dispersion curves for (a) step-index and triangular refractive index profile fibers; (b) depressed cladding fiber.

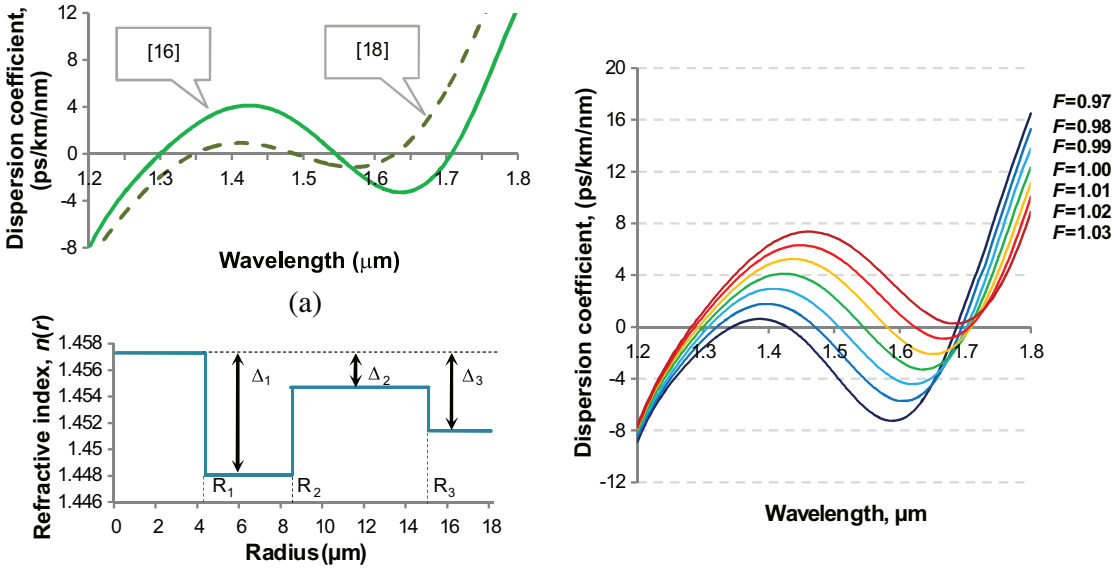

(a) (b) (c)

Figure 3. (a) Dispersion curves for triple-clad fibers with undoped core and fluorine-doped claddings designed in [16] (in light green color) and [18] (dashed dark green curve); (b) schematic refractive index profile of the triple-clad fiber from [16]; (c) dispersion curves for the triple-clad fiber for different scale factor, F.

method. The dispersion curves are depicted in Figure 3(c) and fully concur with the graphs in Figure 2 of [16]. When $F = 1$, the initial graph in Figure 3(a) (in light green color) can be obtained. As can be seen from Figure 3(c), the second zero-dispersion wavelength is much more sensitive to the drawing ratio than the first and third one.

It must be noted that this example has already been used in [2, 6] to test their methods and a deviation of the results obtained in [2] from those in [16] was indicated in [6] with the supposition that the deviation may be credited to the choice of basis functions. However, we use the same basis functions as in [2] but unlike [6] we do not observe their deviation which allows us to say that the discrepancy in the results between [2, 16] is not likely to be related to the choice of basis functions.

d) Based on this example, further optimization was considered in [18] to achieve a more flattened dispersion curve. The optimized parameters for this fiber are: $\Delta_1 = 0.56\%$, $\Delta_2 = 0.17\%$, $\Delta_3 = 0.40\%$, $R_1 = 4.106\,\mu\text{m}$, $R_2 = 8.133\,\mu\text{m}$ and $R_3 = 14.60\,\mu\text{m}$. We calculated the dispersion curve that one would obtain using these parameter values and obtained the dashed dark green curve shown in Figure 3(a) which is indistinguishable from the curve plotted in Figure 4 of [18].

3.2. Analysis of the Convergence and Accuracy of the Proposed Method

3.2.1. Convergence

Figures 4(a) and 4(b) display the change in the normalized propagation coefficient

$$B_N = \left\{ \left((\beta/k_0)^2 - n_{cl}^2 \right) / \left(n_{co}^2 - n_{cl}^2 \right) \right\}^{1/2} \tag{25}$$

for truncated parabolic and step-index profiles with increasing numbers of basis functions, N, in the Galerkin method and show very fast convergence of the values. The slightly better convergence in the case of the truncated parabolic profile is expected as Laguerre-Gauss polynomials, which are used as the basis elements, are the eigenfunctions for the infinitely extended parabolic index profile in circular waveguides. Figure 4(c) shows the convergence of the normalized propagation coefficients for different values of the normalized frequency, V, in the case of step-index fibers. The dashed lines correspond to the values of the normalized propagation coefficient deduced from the exact solution of the scalar wave equation or defined as a high-precision approximation of the solution [25, 42, 43]. It must be noted

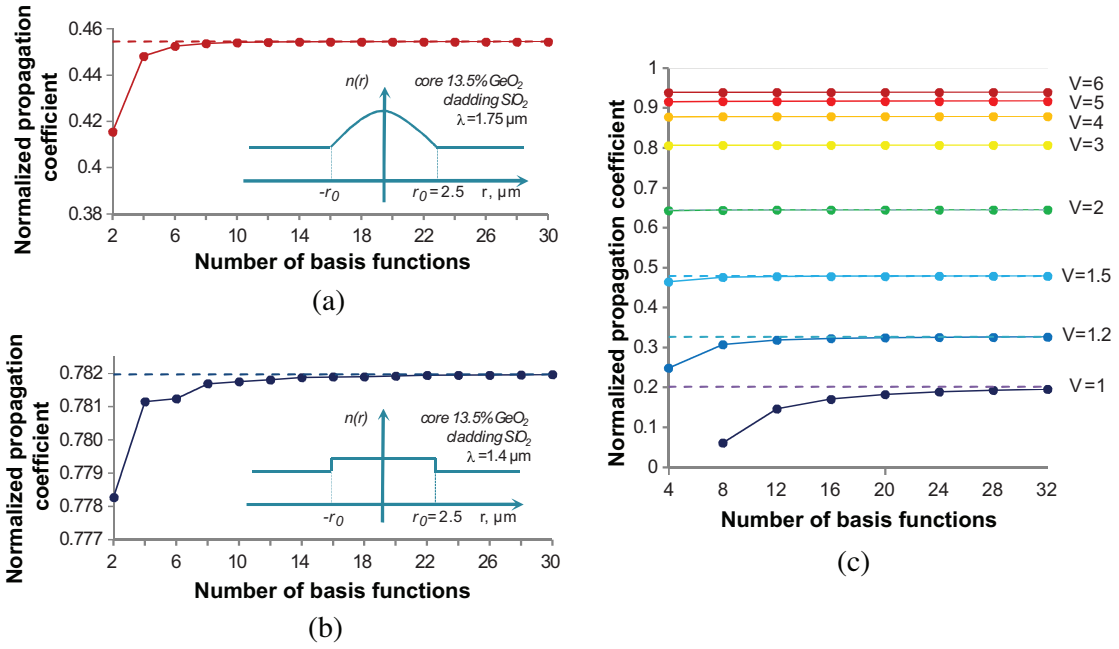

Figure 4. Normalized propagation coefficient plotted as a function of the number of basis functions for: (a) truncated parabolic refractive index profile fiber; (b) step-index fiber; (c) step-index fibers with different values of V.

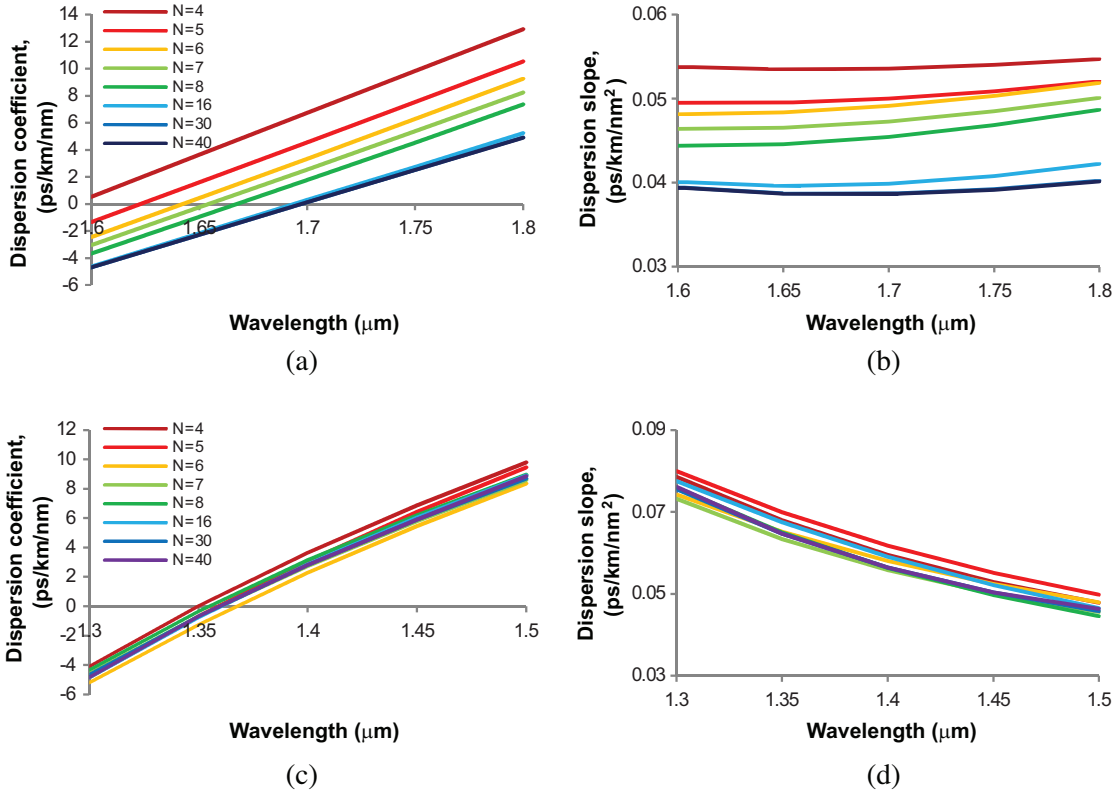

Figure 5. (a) Dispersion and (b) dispersion slope for the truncated parabolic profile fiber from Figure 4(a); (c) dispersion and (d) dispersion slope for the step-index profile fiber from Figure 4(b).

here that the higher the value of V (for progressively single, few or multimode fibers), the better the approximation of the guided modes by means of the Laguerre-Gauss basis functions. The cut-off value of V for single-mode propagation in a fiber depends on the fiber's refractive index profile, in particular, $V \leq 2.405$ for step-index profile and $V \leq 3.518$ for truncated parabolic profile. As a good compromise between accuracy and computation time for these fibers, values of N, the number of basis functions used in the expansion, in the range 16 to 28 can be chosen except for the cases when V is less than 1.2 in which case N must be more than 28 (in fact, in the case when $V < 1.4$, less than half of the modal power propagates in the core of the fiber [44]).

These guidelines for the number of basis functions are also valid for the computation of dispersion and dispersion slope. The convergence of dispersion and dispersion slope values for the truncated parabolic refractive index and step-index fibers from Figure 4 is shown in Figure 5. It must be noted that for the truncated parabolic index profile fiber, Figures 5(a), 5(b), the dispersion and dispersion slope values converge monotonically, which is not the case for the step-index fiber, Figures 5(c), 5(d), although compared to the truncated parabolic index profile fiber a better approximation of dispersion characteristics is obtained for the step-index fiber even when N is as small as 4. In Subsection 3.3, we will discuss the convergence of the propagation coefficient and the dispersion characteristics of step-index fibers to exact solutions.

The computation time for all series of dispersion and dispersion slope values in the two graphs in Figures 5(a), 5(b) for λ changing from 1.6 μm to 1.8 μm in steps of 0.05 μm for the number of basis functions $N = 16$ is 0.09 s (the time is for all 10 values together: 5 values of dispersion and 5 values of dispersion slope). The calculations were performed on an Intel Pentium (R) CPU 2 GHz.

Figure 6 compares the values of waveguide dispersion, D_w, as a function of wavelength computed using the present method with those obtained using numerical differentiation of the propagation coefficient in [3] for the same step-index single-mode fiber. The refractive index profile of the fiber is embedded in the graph in Figure 6(a). In [3], Bessel functions were used as the basis elements for

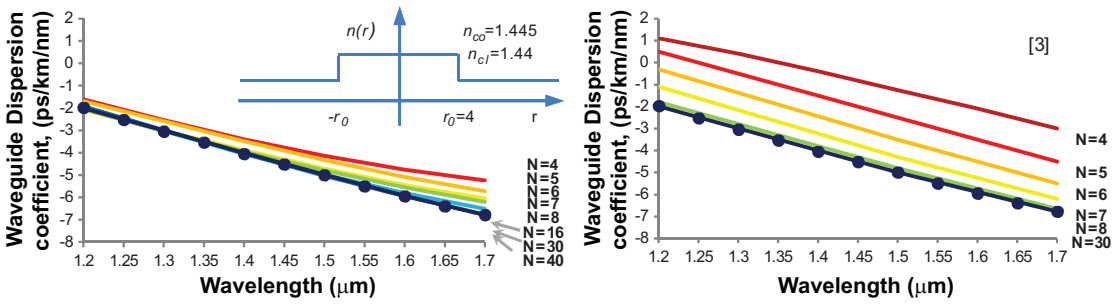

(a) (b)

Figure 6. Waveguide dispersion for a step-index fiber: (a) present method; (b) Galerkin method with Bessel functions and numerical differentiation [3] by the finite difference method.

the Galerkin method. The graphs show that both methods rapidly converge to the exact solution (the line with solid circles [3]). Although Bessel functions represent the eigenmodes for step-index profile fibers, our calculation method exhibits better convergence which must be attributed to the analytical differentiation of the matrix equation as opposed to numerical differentiation in [3]. This agrees with the results shown in Figure 5(c) when for a step-index fiber sufficiently good approximations of the dispersion values can be obtained even for N as small as 4.

3.2.2. Accuracy

The modeled values of propagation coefficient, group delay, dispersion and dispersion slope for a truncated parabolic refractive index profile fiber when the matrix size increases, due to increased numbers of basis functions in the expansion, are tabulated in Table 1. The fiber design is the same as that previously considered in [2, 6], and to aid comparison, the dispersion values determined in [2, 6] are included in the table. The method for dispersion calculation in [6] is based on a variational finite-element formulation and quite different from our approach. It is difficult to compare these two methods as computing approximate values is always a trade-off between accuracy and computation time, consequently information about the computation time for the method in [6] must be taken into account for a proper comparison which was not given in [6]. In the present method, the computation time for the values of the propagation coefficient, group delay, dispersion and dispersion slope in Table 1 for $N = 25$, 35 and 45 was 0.059 s, 0.195 s and 0.4 s respectively (Intel Pentium (R) CPU 2 GHz).

Table 1. Convergence of propagation coefficient, group delay, dispersion and dispersion slope values with increasing numbers of basis functions.

Truncated parabolic profile core: 13.5% GeO_2, 86.5% SiO_2, *cladding*: *pure* SiO_2, *core radius:* 2.5 μm, $\lambda = 1.75$ μm				
Matrix size, N	**Effective propagation coefficient, β/k_0**	**Group delay, τ_g (ns/km)**	**Dispersion, D (ps/nm/km)**	**Dispersion slope, DS (ns/nm^2/km)**
5	1.44627916	4.93459345	7.54688736	0.05960322
15	1.44635525	4.93317160	2.80932819	0.05017661
25	1.44635615	4.93313637	2.54241550	0.04803728
35	1.44635620	4.93313384	2.51601666	0.04801827
45,	1.44635631	4.93313348	2.50867604	0.04797553
[2] $N = 35$,			2.5169	
[6], 7 elements			2.510856	

Table 2. Comparison of dispersion values (ps/nm/km) and corresponding computation time for different calculation methods.

Matrix size, N	Present method	A. Sharma, S. Banerjee [2]	Finite difference method	
			h=0.1 μm	h=0.01 μm
Step-index profile core: 13.5% GeO_2, 86.5% SiO_2, *cladding: pure* SiO_2, *core radius:* 2.5 μm, λ = 1.4 μm				
10	2.7962 (0.016s)	2.8068 (-)	2.7977 (0.03s)	2.8019 (0.03s)
15	2.7930 (0.025s)	2.7993 (-)	2.7957 (0.06s)	2.7509 (0.08s)
20	2.7947 (0.032s)	2.7969 (-)	2.7946 (0.11s)	2.2571 (0.12s)
25	2.7880(0.058s)	2.7916 (-)	2.7866 (0.20s)	2.8409 (0.22s)
Truncated parabolic index profile core: 13.5% GeO_2, 86.5% SiO_2, *cladding: pure* SiO_2, *core radius:* 2.5 μm, λ = 1.75 μm				
20	2.6008 (0.032s)	2.6685 (-)	2.6132 (0.12s)	3.0160 (0.13s)
25	2.5424 (0.059s)	2.5614 (-)	2.5422 (0.20s)	3.0646 (0.22s)
30	2.5220 (0.112s)	2.5287 (-)	2.5266 (0.34s)	3.0160 (0.34s)
35	2.5160 (0.195s)	2.5169 (-)	2.5062 (0.52s)	2.2863 (0.53s)

The present method yields values for dispersion for $N = 35$ of the same order as those for [2], however, the present method continues to converge monotonically below what may be considered to have been the best approximate value [6] until now.

In [2] the dispersion is found using matrix perturbation theory while the scalar wave equation is solved using the Rayleigh-Ritz procedure with Laguerre-Gauss basis functions. As the Galerkin method, which is used in our approach, is identical to the Rayleigh-Ritz variational method [24], the difference in dispersion values is due to the difference in the techniques to differentiate the propagation coefficient. Table 2 provides a more detailed comparison of the two differentiation approaches for step-index and truncated parabolic profile fibers in the second and third columns. It must be noted again that the dispersion values are of the same order, however, for proper comparison, the computation time must be taken into account. The dispersion values have also been determined by numerical differentiation using the finite difference method, which are also provided in Table 2. Five equidistant wavelengths were used to calculate the second order derivative of the propagation coefficient. Different step sizes, h, were considered for numerical differentiation. The corresponding computation time for each value in our method and in the finite difference method is indicated in parentheses (a hyphen means the computation time is not available). Both methods were run on the same computer. As expected, the table shows that the present method has an advantage both in terms of accuracy (as it does not approximate the derivatives while there are always errors inherent in the finite difference method) and in terms of computation time: the present method is 2–3 times faster than the finite difference method in which the eigenvalue problem is solved five times against three times in the proposed approach to calculate dispersion values. Numerical differentiation for second order derivatives based on three points which requires solving the eigenvalue equation three times gives even worse accuracy. In addition, three points are not enough to approximate the third order derivatives.

3.3. Comparison of Numerical Results with Exact Solutions Available for Step-Index Fibers

The exact solutions for weakly-guiding step-index optical fibers for various values of the normalized frequency, V, are provided in [37]. Table 3 compares the simulation results for the effective propagation coefficient, group delay and the waveguide dispersion with corresponding exact data. As can be seen from the table, for the number of basis functions $N = 16$ or more, the relative error, (exact_value-numerical_result)/exact_value, is within 1E-06, 5E-06, and 2E-02 for the effective propagation coefficient, group delay and the waveguide dispersion correspondingly. Plots of convergence of the simulated data

Table 3. Comparison of numerical results with exact data for weakly-guiding step-index fibers.

V	***Exact value***	***N*=4**	*relative error*	***N*=16**	*relative error*	***N*=32**	*relative error*
			Effective propagation coefficient				
1.5	1.456431	1.456406	1.7E-05	1.456431	2.1E-07	1.456431	−8.9E-08
2.5	1.458890	1.458884	4.2E-06	1.458890	1.1E-07	1.458891	−2.5E-07
3.5	1.463368	1.463350	1.3E-05	1.463367	9.1E-07	1.463368	1.0E-07
			Group delay				
1.5	4.862017	4.862427	−8.4E-05	4.862029	−2.5E-06	4.862019	−3.0E-07
2.5	4.876357	4.876360	−6.0E-07	4.876364	−1.5E-06	4.876367	−2.1E-06
3.5	4.895396	4.895263	2.7E-05	4.895417	−4.3E-06	4.895414	−3.6E-06
			Waveguide dispersion (λ=1.55 μm)				
1.5	−4.293057	−2.888118	3.3E-01	4.219240	1.7E-02	−4.299048	−1.4E-03
2.5	−1.680499	−1.371568	1.8E-01	1.649684	1.8E-02	−1.677112	2.0E-03
3.5	1.485910	1. 418160	4.6E-02	1.478307	5.1E-03	1.492531	−4.5E-03

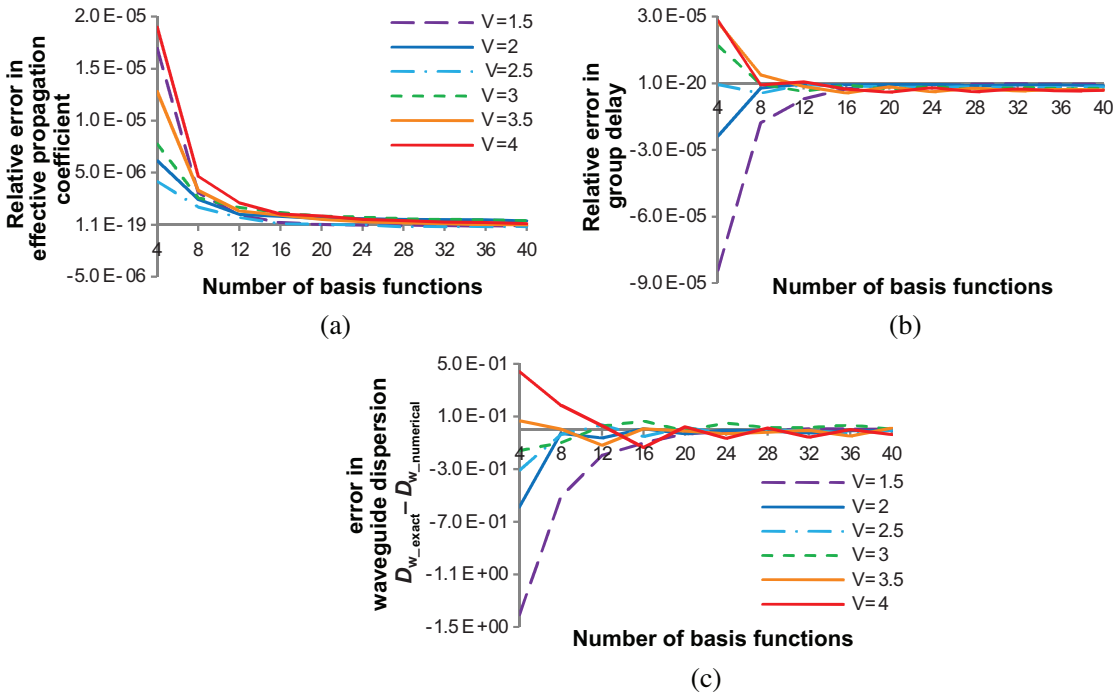

Figure 7. Plots of errors in the propagation and dispersion characteristics for step-index fibers: (a) relative error in the effective propagation coefficient; (b) relative error in the group delay; (c) errors in waveguide dispersion values, $D_{w\_exact} - D_{w\_numerical}$.

for these parameters against the increasing number of basis functions are shown in Figure 7. As has been noted in Subsection 3.2, unlike the case of the truncated parabolic index profile fiber when the dispersion values converge monotonically, for step-index fibers we observe slight oscillations in the dispersion parameters values.

3.4. Comparison of Total Dispersion, D, with the Approximation $D_w + D_m$

The total dispersion was calculated using Equation (2) and the waveguide and material dispersion parameters were separately calculated. Figures 8 and 9 compare the total chromatic dispersion, D, with the sum of the waveguide dispersion, D_w, and material dispersion, D_m for step-index and parabolic index profile fibers with GeO_2-doped core (13.5%) and pure SiO_2 cladding for a range of different core radii. Determination of the real material dispersion for an arbitrary refractive index profile structure is rather complicated. In practice, for the sake of simplicity, only the core or cladding material dispersion is usually taken into account. The waveguide dispersion is calculated assuming that the core and cladding media are independent of wavelength.

Figures 8(a) and 9(a) show the effective propagation coefficient, $n_{eff} = \beta/k_0$, for each of the fiber designs, where curves which suddenly stop short in the cases $r_0 = 1\,\mu m$ and $1.5\,\mu m$ indicate that the modes go beyond cut-off so that there are no guided modes in the fibers after certain values of wavelength. The solid circles indicate that single-mode propagation occurs at wavelengths longer than the marked one while at wavelengths to the left of the solid circles the fiber has more than one guided mode representing few-mode fiber operation. The waveguide dispersion, D_w, is plotted in Figures 8(b) and 9(b) for step-index and parabolic index profile fibers respectively, together with the material dispersion of the core, D_m, but with the opposite sign, $-D_m$, to illustrate at which wavelengths the total dispersion becomes zero which is when the inverted material dispersion cuts the waveguide dispersion curves. Figures 8(c) and 9(c) depict the total dispersion curves, D, defined using Equation (2) for step-index and parabolic index profile fibers respectively while the dispersion curves for these fibers defined using the approximation $D_m + D_w$ are shown in Figures 8(d) and 9(d). By comparing the dispersion curves in Figure 8(c), with those in Figure 8(d) and the curves in Figure 9(c) with those in Figure 9(d), the dispersion curves obtained from the sum $D_w + D_m$ can be seen to give a reasonable approximation to those found using Equation (2). However, it must be noted that

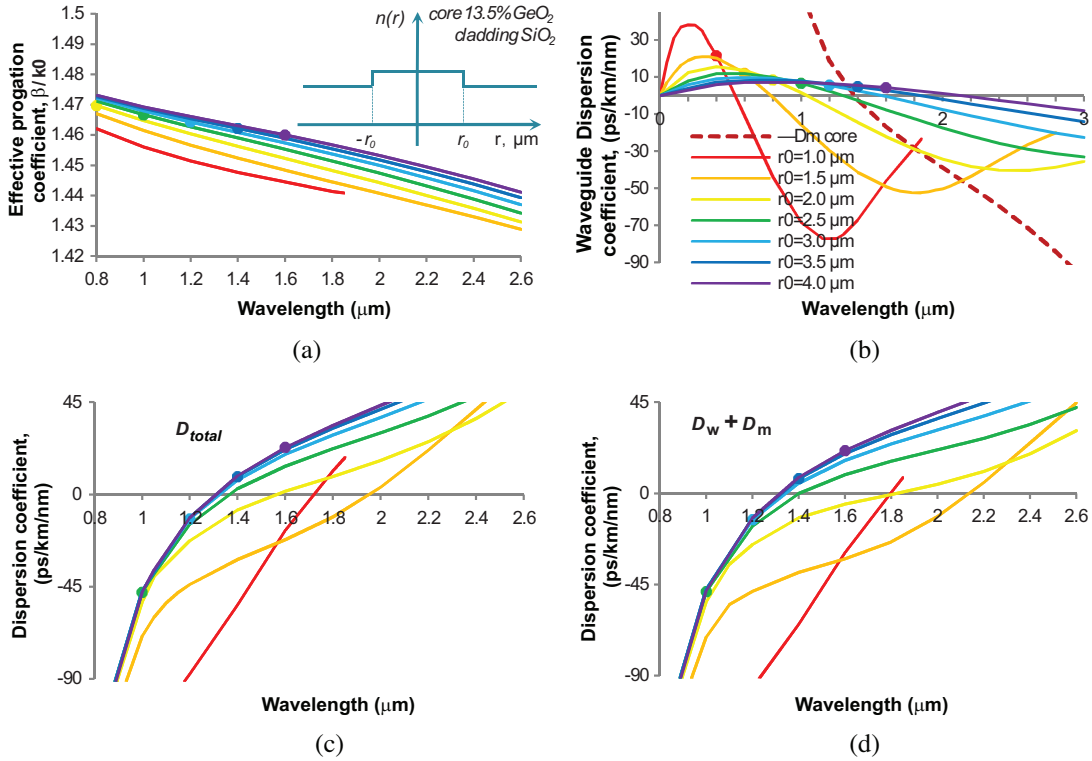

Figure 8. Comparison of total chromatic dispersion of step index fibers with different core radii defined in two ways: (a) effective propagation coefficient $n_{eff} = \beta/k_0$ for the corresponding fibers; (b) waveguide, D_w, and material, D_m, dispersion curves; (c) D defined using Equation (2) and (d) as the sum of waveguide and material dispersion $D_w + D_m$.

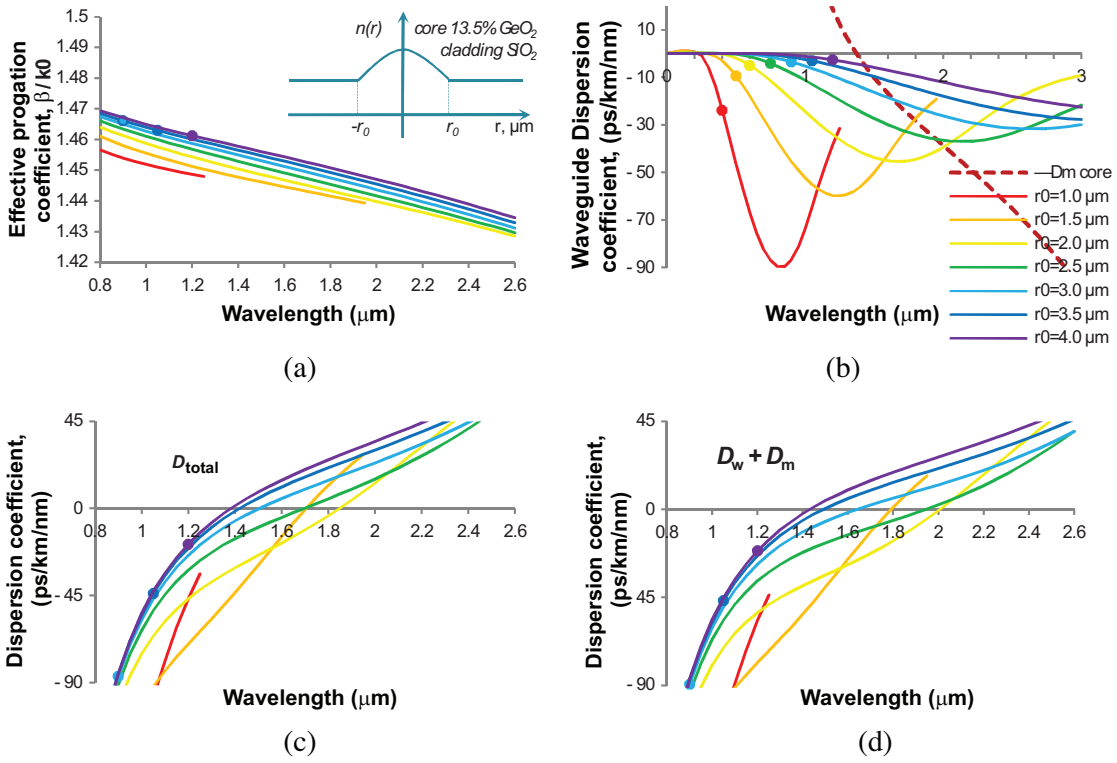

Figure 9. Comparison of total chromatic dispersion of parabolic index profile fibers with different core radii defined in two ways: (a) effective propagation coefficient $n_{eff} = \beta/k_0$ for the corresponding fibers; (b) waveguide, D_w, and material, D_m, dispersion curves; (c) D defined using Equation (2) and (d) as the sum of waveguide and material dispersion $D_w + D_m$.

although the approximation is better for higher radii values there is still a significant difference between the corresponding dispersion values in the case of smaller radii and at longer wavelengths even in the case of larger radii. This discrepancy between the total dispersion, D, and the sum $D_w + D_m$, can be taken into account by including an additional term, a profile dispersion parameter, D_P, which is proportional to $d\Delta/d\lambda$ [45, 46]. The difference between the total dispersion and the sum $D_w + D_m$ is plotted in Figures 10(a) and (b) for step-index and parabolic index profile fibers respectively. The graphs are similar to those of the profile dispersion in Figures 6(c) and 7(c) from [46]. As can be seen from Figures 10(a) and (b), the use of the sum $D_w + D_m$ to approximate the dispersion values can give an absolute error up to 10 ps/(nm·km) in both cases of step-index and parabolic index fibers. For long haul communication systems and high precision systems a higher degree of accuracy is required for the calculation of dispersion parameters than that provided by the sum, $D_w + D_m$.

4. CONCLUSION

A method for accurate and fast calculation of the group delay, dispersion and dispersion slope of single-mode weakly guiding optical fibers with radially arbitrary refractive index profile has been introduced which relies on analytical differentiation of the propagation coefficient. The model incorporates the wavelength dependent nature of the core and cladding materials producing total chromatic dispersion parameters for optical fibers. The method also conveniently allows the waveguide and material dispersion to be considered separately. The results are thoroughly compared to available exact and experimental data to validate the method. Comparison to other calculation techniques shows it to be more accurate whilst providing faster convergence, faster calculation speed to aid fiber dispersion design. The method is demonstrated for parabolic, triangular and step index, single-clad, double-clad, and triple-clad optical fibers.

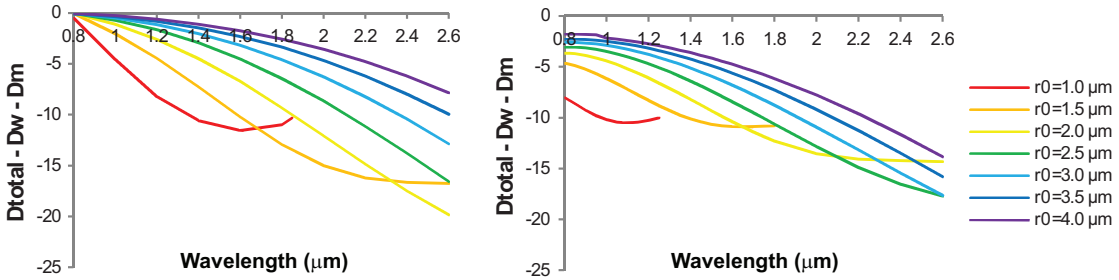

(a) (b)

Figure 10. Difference between the total chromatic dispersion defined using Equation (2) and as the sum of waveguide and material dispersion $D_w + D_m$: (a) step index fiber; (b) parabolic index fiber with different core radii.

ACKNOWLEDGMENT

Raushan Mussina gratefully acknowledges the support of the Republic of Kazakhstan via the Bolashak Scholarship Programme and the European Union via the Erasmus Mundus External Cooperation Window Mobility Grant Programme.

APPENDIX A. THE DERIVATIVES OF THE MATRIX ELEMENTS

For the sake of convenience, in this section differentiation is done with respect to scaled frequency $\tilde{\omega}$, defined as $\tilde{\omega} = \omega r_0/c = 2\pi r_0/\lambda$ and, for brevity, we replace derivatives by a prime, $'$. The differentiation can be done in different ways depending on how the expressions are grouped. One way is presented here.

$$a_{ij} = K^m_{(i-1)(j-1)}\left(I^m_{(i-1)(j-1)} + J^m_{(i-1)(j-1)}\right) + \beta_0^2\delta_{i,j} \tag{A1}$$

$$(a_{ij})' = \left(K^m_{(i-1)(j-1)}\right)'\left(I^m_{(i-1)(j-1)} + J^m_{(i-1)(j-1)}\right) + K^m_{(i-1)(j-1)}\left(\left(I^m_{(i-1)(j-1)}\right)' + \left(J^m_{(i-1)(j-1)}\right)'\right) + \left(\beta_0^2\right)'\delta_{i,j} \tag{A2}$$

$$(a_{ij})'' = \left(K^m_{(i-1)(j-1)}\right)''\left(I^m_{(i-1)(j-1)} + J^m_{(i-1)(j-1)}\right) + 2\left(K^m_{(i-1)(j-1)}\right)'\left(\left(I^m_{(i-1)(j-1)}\right)' + \left(J^m_{(i-1)(j-1)}\right)'\right)$$
$$+ K^m_{(i-1)(j-1)}\left(\left(I^m_{(i-1)(j-1)}\right)'' + \left(J^m_{(i-1)(j-1)}\right)''\right) + \left(\beta_0^2\right)''\delta_{i,j} \tag{A3}$$

$$(a_{ij})''' = \left(K^m_{(i-1)(j-1)}\right)'''\left(I^m_{(i-1)(j-1)} + J^m_{(i-1)(j-1)}\right) + 3\left(K^m_{(i-1)(j-1)}\right)''\left(\left(I^m_{(i-1)(j-1)}\right)' + \left(J^m_{(i-1)(j-1)}\right)'\right)$$
$$+3\left(K^m_{(i-1)(j-1)}\right)'\left(\left(I^m_{(i-1)(j-1)}\right)'' + \left(J^m_{(i-1)(j-1)}\right)''\right) + K^m_{(i-1)(j-1)}\left(\left(I^m_{(i-1)(j-1)}\right)''' + \left(J^m_{(i-1)(j-1)}\right)'''\right) + \left(\beta_0^2\right)'''\delta_{i,j} \tag{A4}$$

$$\beta_0^2 = k_0^2 n_{co}^2\left[1 - 2\Delta\frac{2n+m+1}{V/2}\right] = k_0^2 n_{co}^2 - 2(2n+m+1)\frac{k_0}{r_0}\sqrt{n_{co}^2 - n_{cl}^2} \tag{A5}$$

$$\left(\beta_0^2\right)' = 2k_0 n_{co}^2/r_0 + k_0^2\left(n_{co}^2\right)' - 2\left(2n+m+1\right)\sqrt{n_{co}^2 - n_{cl}^2}\Big/r_0^2 - 2\left(2n+m+1\right)k_0\left(\sqrt{n_{co}^2 - n_{cl}^2}\right)'\Big/r_0 \tag{A6}$$

$$\left(\beta_0^2\right)'' = 2n_{co}^2/r_0^2 + 4k_0\left(n_{co}^2\right)'/r_0 + k_0^2\left(n_{co}^2\right)'' - 4\left(2n+m+1\right)\left(\sqrt{n_{co}^2 - n_{cl}^2}\right)'\Big/r_0^2$$
$$-2\left(2n+m+1\right)k_0\left(\sqrt{n_{co}^2 - n_{cl}^2}\right)''\Big/r_0 \tag{A7}$$

$$\left(\beta_0^2\right)''' = 6\left(n_{co}^2\right)'/r_0^2 + 6k_0\left(n_{co}^2\right)''/r_0 + k_0^2\left(n_{co}^2\right)''' - 6\left(2n+m+1\right)\left(\sqrt{n_{co}^2-n_{cl}^2}\right)''\Big/r_0^2$$
$$-2\left(2n+m+1\right)k_0\left(\sqrt{n_{co}^2-n_{cl}^2}\right)'''\Big/r_0 \tag{A8}$$

For n_{co} and n_{cl}:

$$n^2 = 1+\sum_{i=1}^{3}\frac{\alpha_i\lambda^2}{\lambda^2-l_i^2} = 1+\sum_{i=1}^{3}\frac{A_iB_i}{B_i-\tilde{\omega}^2}, \qquad A_i=\alpha_i, \qquad B_i=\frac{4\pi^2r_0^2}{l_i^2} \tag{A9}$$

$$\left(n^2\right)' = \sum_{i=1}^{3}\frac{2A_iB_i\tilde{\omega}}{\left(B_i-\tilde{\omega}^2\right)^2} \tag{A10}$$

$$\left(n^2\right)'' = \sum_{i=1}^{3}\frac{2A_iB_i\left(B_i+3\tilde{\omega}^2\right)}{\left(B_i-\tilde{\omega}^2\right)^3} \tag{A11}$$

$$\left(n^2\right)''' = 24\sum_{i=1}^{3}\frac{A_iB_i^2\tilde{\omega}+A_iB_i\tilde{\omega}^3}{\left(B_i-\tilde{\omega}^2\right)^4} \tag{A12}$$

$$\left(\sqrt{n_{co}^2-n_{cl}^2}\right)' = \frac{\left(n_{co}^2\right)'-\left(n_{cl}^2\right)'}{2\sqrt{n_{co}^2-n_{cl}^2}} \tag{A13}$$

$$\left(\sqrt{n_{co}^2-n_{cl}^2}\right)'' = -\frac{\left(\left(n_{co}^2-n_{cl}^2\right)'\right)^2}{4\left(\sqrt{n_{co}^2-n_{cl}^2}\right)^3}+\frac{\left(n_{co}^2\right)''-\left(n_{cl}^2\right)''}{2\sqrt{n_{co}^2-n_{cl}^2}} \tag{A14}$$

$$\left(\sqrt{n_{co}^2-n_{cl}^2}\right)''' = \frac{3\left(\left(n_{co}^2-n_{cl}^2\right)'\right)^3}{8\left(\sqrt{n_{co}^2-n_{cl}^2}\right)^5}-\frac{3\left(n_{co}^2-n_{cl}^2\right)'\left(\left(n_{co}^2\right)''-\left(n_{cl}^2\right)''\right)}{4\left(\sqrt{n_{co}^2-n_{cl}^2}\right)^3}+\frac{\left(n_{co}^2\right)'''-\left(n_{cl}^2\right)'''}{2\sqrt{n_{co}^2-n_{cl}^2}} \tag{A15}$$

$$K_{ij}^m = 2\Delta k_0^2n_{co}^2\left[\frac{(i+m)!}{i!}\frac{(j+m)!}{j!}\right]^{-1/2} = \gamma k_0^2\left(n_{co}^2-n_{cl}^2\right),$$
$$\gamma = \left[\frac{(i+m)!}{i!}\frac{(j+m)!}{j!}\right]^{-1/2} \tag{A16}$$

$$\left(K_{ij}^m\right)' = \gamma\left(2k_0\left(n_{co}^2-n_{cl}^2\right)/r_0+k_0^2\left(n_{co}^2-n_{cl}^2\right)'\right) \tag{A17}$$

$$\left(K_{ij}^m\right)'' = \gamma\left(2\left(n_{co}^2-n_{cl}^2\right)/r_0^2+4k_0\left(n_{co}^2-n_{cl}^2\right)'/r_0+k_0^2\left(n_{co}^2-n_{cl}^2\right)''\right) \tag{A18}$$

$$\left(K_{ij}^m\right)''' = \gamma\left(6\left(n_{co}^2-n_{cl}^2\right)'/r_0^2+6k_0\left(n_{co}^2-n_{cl}^2\right)''/r_0+k_0^2\left(n_{co}^2-n_{cl}^2\right)'''\right) \tag{A19}$$

$$J_{ij}^m = \int_0^\infty e^{-x}x^mL_i^m\left(x\right)\left[x/V-1\right]L_j^m\left(x\right)dx = \frac{1}{V}\Theta_1-\Theta_2 \tag{A20}$$

where Θ_1 and Θ_2 are constants:

$$\Theta_1 = \int_0^\infty e^{-x}x^{m+1}L_i^m\left(x\right)L_j^m\left(x\right)dx,$$
$$\Theta_2 = \int_0^\infty e^{-x}x^mL_i^m\left(x\right)L_j^m\left(x\right)dx \tag{A21}$$

$$\left(J_{ij}^m\right)' = -\frac{V'}{V^2}\Theta_1 \tag{A22}$$

$$\left(J_{ij}^{m}\right)'' = \left(2\frac{(V')^2}{V^3} - \frac{V''}{V^2}\right)\Theta_1 \tag{A23}$$

$$\left(J_{ij}^{m}\right)''' = \left(-6\frac{(V')^3}{V^4} + 6\frac{V'V''}{V^3} - \frac{V'''}{V^2}\right)\Theta_1 \tag{A24}$$

$$I_{ij}^{m} = \int_0^V e^{-x}x^m L_i^m(x)\left[1 - f\left(\sqrt{x/V}\right)\right]L_j^m(x)\,dx \tag{A25}$$

In Equations (A26)–(A28), $\dot{f}$, $\ddot{f}$ and $\dddot{f}$ denote the derivatives of f with respect to its argument.

$$\left(I_{ij}^{m}\right)' = V'e^{-V}V^m L_i^m(V)\,L_j^m(V)\,[1 - f_{\text{-}}(1)] + \frac{V'}{2(\sqrt{V})^3}\int_0^V e^{-x}x^{m+\frac{1}{2}}L_i^m(x)L_j^m(x)\dot{f}\left(\sqrt{x/V}\right)dx \tag{A26}$$

here $f_{\text{-}}(1)$ is $\lim f(r/r_0)$ when $r \to r_0$ from the left

$$\begin{aligned}\left(I_{ij}^{m}\right)'' &= \left(V'' - \left(V'\right)^2 + \frac{m\left(V'\right)^2}{V}\right)e^{-V}V^m L_i^m(V)L_j^m(V)\,[1 - f_{\text{-}}(1)] + \frac{(V')^2}{2(\sqrt{V})^3}e^{-V}V^{m+\frac{1}{2}}L_i^m(V)\\ &\times L_j^m(V)\,\dot{f}_{\text{-}}(1) - \left(V'\right)^2 e^{-V}V^m\,[1 - f_{\text{-}}(1)]\left(L_{i-1}^{m+1}(V)\,L_j^m(V) + L_i^m(V)\,L_{j-1}^{m+1}(V)\right)\\ &+ \left(\frac{V''}{2(\sqrt{V})^3} - \frac{3\left(V'\right)^2}{4(\sqrt{V})^5}\right)\int_0^V e^{-x}x^{m+\frac{1}{2}}L_i^m(x)L_j^m(x)\,\dot{f}\left(\sqrt{x/V}\right)dx\\ &- \frac{(V')^2}{4V^3}\int_0^V e^{-x}x^{m+1}L_i^m(x)L_j^m(x)\,\ddot{f}\left(\sqrt{x/V}\right)dx\end{aligned} \tag{A27}$$

$$\begin{aligned}\left(I_{ij}^{m}\right)''' &= \left(V''' - 3V'V'' + \left(V'\right)^3 + \frac{3mV'V''}{V} - \frac{2m\left(V'\right)^3}{V} - \frac{m\left(V'\right)^3}{V^2} + \frac{m^2(V')^3}{V^2}\right)e^{-V}V^m L_i^m(V)\\ &\times L_j^m(V)\,[1 - f_{\text{-}}(1)] - \left(3V'V'' - 2\left(V'\right)^3 + \frac{2m\left(V'\right)^3}{V}\right)e^{-V}V^m\,[1 - f_{\text{-}}(1)]\\ &\times\left(L_{i-1}^{m+1}(V)\,L_j^m(V) + L_i^m(V)\,L_{j-1}^{m+1}(V)\right) + \left(V'\right)^3 e^{-V}V^m\,[1 - f_{\text{-}}(1)]\\ &\times\left(L_{i-2}^{m+2}(V)\,L_j^m(V) + L_{i-1}^{m+1}(V)\,L_{j-1}^{m+1}(V) + L_{i-1}^{m+1}(V)\,L_{j-1}^{m+1}(V) + L_i^m(V)\,L_{j-2}^{m+2}(V)\right)\\ &+ \left(\frac{3V'V''}{2(\sqrt{V})^3} - \frac{3\left(V'\right)^3}{2(\sqrt{V})^5} - \frac{(V')^3}{2(\sqrt{V})^3} + \frac{(2m+1)\left(V'\right)^3}{4V(\sqrt{V})^3}\right)e^{-V}V^{m+\frac{1}{2}}L_i^m(V)\,L_j^m(V)\,\dot{f}_{\text{-}}(1)\\ &- \frac{(V')^3}{2(\sqrt{V})^3}e^{-V}V^{m+\frac{1}{2}}\dot{f}_{\text{-}}(1)\left(L_{i-1}^{m+1}(V)\,L_j^m(V) + L_i^m(V)\,L_{j-1}^{m+1}(V)\right) - \frac{(V')^3}{4V^3}e^{-V}V^{m+1}\\ &\times L_i^m(V)\,L_j^m(V)\,\ddot{f}_{\text{-}}(1) + \left(-\frac{9V'V''}{4(\sqrt{V})^5} + \frac{V'''}{2(\sqrt{V})^3} + \frac{15\left(V'\right)^3}{8(\sqrt{V})^7}\right)\int_0^V e^{-x}x^{m+\frac{1}{2}}L_i^m(x)L_j^m(x)\\ &\times\dot{f}\left(\sqrt{x/V}\right)dx + \left(-\frac{3V'V''}{4V^3} + \frac{9\left(V'\right)^3}{8V^4}\right)\int_0^V e^{-x}x^{m+1}L_i^m(x)L_j^m(x)\ddot{f}\left(\sqrt{x/V}\right)dx\\ &+ \frac{(V')^3}{8\left(\sqrt{V}\right)^9}\int_0^V e^{-x}x^{m+\frac{3}{2}}L_i^m(x)L_j^m(x)\dddot{f}\left(\sqrt{x/V}\right)dx\end{aligned} \tag{A28}$$

$$V = k_0 r_0\sqrt{n_{co}^2 - n_{cl}^2} \tag{A29}$$

$$V' = \sqrt{n_{co}^2 - n_{cl}^2} + k_0 r_0\left(\sqrt{n_{co}^2 - n_{cl}^2}\right)' \tag{A30}$$

$$V'' = 2\left(\sqrt{n_{co}^2 - n_{cl}^2}\right)' + k_0 r_0 \left(\sqrt{n_{co}^2 - n_{cl}^2}\right)'' \tag{A31}$$

$$V''' = 3\left(\sqrt{n_{co}^2 - n_{cl}^2}\right)'' + k_0 r_0 \left(\sqrt{n_{co}^2 - n_{cl}^2}\right)''' \tag{A32}$$

Then, the group delay, τ_g, dispersion, D, and the dispersion slope, DS, are expressed in terms of $\tilde{\omega}$ as follows:

$$\tau_g = \frac{d\beta}{d\omega} = \frac{r_0}{c}\frac{d\beta}{d\tilde{\omega}} \quad \text{or} \quad \tau_g = \frac{r_0}{c}\beta' \tag{A33}$$

$$D = -\frac{\tilde{\omega}^2}{2\pi c}\beta'' \tag{A34}$$

$$DS = \frac{r_0\tilde{\omega}}{c\lambda^2}\left(2\beta'' + \tilde{\omega}\beta'''\right) \tag{A35}$$

The expressions for the derivatives of the eigenvalues, β^2, and the propagation coefficient, β, in terms of $\tilde{\omega}$ will remain the same except ω replaced by $\tilde{\omega}$:

$$\left(\beta^2\right)' = \mathbf{c}^T\mathbf{A}'\mathbf{c} \tag{A36}$$

$$\left(\beta^2\right)'' = \mathbf{c}^T\left(\mathbf{A}''\right)\mathbf{c} + 2\mathbf{c}^T\mathbf{A}'\mathbf{c}' \tag{A37}$$

$$\left(\beta^2\right)''' = \mathbf{c}^T\mathbf{A}'''\mathbf{c} + 3\mathbf{c}^T\mathbf{A}''\mathbf{c}' + 3\mathbf{c}^T\left(\mathbf{A}' - \left(\beta^2\right)'\mathbf{I}\right)\mathbf{c}'' \tag{A38}$$

$$\beta' = \frac{1}{2\beta}\left(\beta^2\right)' \tag{A39}$$

$$\beta'' = \frac{1}{2\beta}\left[\left(\beta^2\right)'' - 2\left(\beta'\right)^2\right] \tag{A40}$$

$$\beta''' = \frac{1}{2\beta}\left[\left(\beta^2\right)''' - 6\beta'\beta''\right] \tag{A41}$$

APPENDIX B. APPLICATION OF THE GALERKIN METHOD TO WEAKLY-GUIDING OPTICAL FIBER MODEL [25]

The transverse electromagnetic fields Ψ of the waves in weakly guiding optical fibers are governed by the scalar wave equation

$$\nabla^2\Psi + k_0^2 n^2(r)\Psi = 0 \tag{B1}$$

with suppressed time dependence $\exp(-i\omega t)$, where k_0 is the free-space wavenumber and $n(r)$ is the refractive index profile of the fiber which only varies in the radial direction. If the direction of propagation is along the z-axis, and β is the propagation coefficient, then Equation (B1) reduces to

$$\left[\nabla_t^2 + k_0^2 n^2(r)\right]\psi(r,\theta) = \beta^2\psi(r,\theta), \tag{B2}$$

where ∇_t^2 is the transverse part of the Laplacian operator.

The refractive index profile is assumed to be independent of θ, then $\psi(r,\theta)$ can be written in terms of constituents of the form:

$$\psi_m(r,\theta) = R_{lm}(r)\exp(-im\theta), \tag{B3}$$

so that the functions $R_{lm}(r)$ satisfy the radial wave equation:

$$\left[\frac{d^2}{dr^2} + \frac{1}{r}\frac{d}{dr} + k_0^2 n^2(r) - \frac{m^2}{r^2} - \beta^2\right]R_{lm}(r) = 0, \tag{B4}$$

where nonnegative l and m are the radial and azimuthal mode numbers, respectively. Below, we shall consider m fixed.

The Galerkin method is applied to solve Equation (B2) with the use of the Laguerre-Gauss polynomials to expand $\psi_m(r,\theta)$

$$\psi_m(r,\theta) = \exp(-im\theta)\sum_{l=0}^{N-1} c_l b_l^m(x(r)), \tag{B5}$$

where $x(r)$ is the normalized radial coordinate defined in Subsection 3.2, and the basis functions $b_l^m(x(r))$ must be chosen such that they satisfy the boundary conditions: they are finite at $r = 0$ and decay to zero as $r \to \infty$. The Laguerre-Gauss polynomials which satisfy these boundary conditions are the eigensolutions of Equation (B4) for an infinitely extended parabolic refractive index profile, $n(r)$, Figure 1(a). They form a complete set of orthonormal functions:

$$b_l^m(x(r)) = \left[\frac{V}{\pi r_0^2}\frac{l!}{(l+m)!}\right]^{1/2}\exp\left(-\frac{x(r)}{2}\right)x(r)^{m/2}L_l^m(x(r)), \quad l = 0,1,2,\ldots,N-1, \tag{B6}$$

where $L_l^m(x)$ are generalized Laguerre polynomials, V is the normalized frequency. Then, the partial differential Equation (B2) can be transformed into an infinite system of linear equations

$$\sum_{j=1}^{\infty}\left[\left\langle b_i^m, \left(\nabla_t^2 + k_0^2 n^2(r)\right) b_j^m\right\rangle - \beta^2\delta_{i,j}\right]c_j = 0, \quad i = l+1 = 1,2,\ldots,N, \tag{B7}$$

where δ_{ij} is the Kronecker delta and

$$\left\langle b_i^m, b_j^m\right\rangle = \int_0^{\infty} b_i^m(x)\cdot b_j^m(x)\,dx = \delta_{ij}. \tag{B8}$$

For finite N, Equation (B7) can be written in matrix form as

$$\mathbf{Ac} = \beta^2\mathbf{c}, \tag{B9}$$

where $\mathbf{A}$ is a real symmetric matrix and

$$\mathbf{A} = \{a_{ij}\} = \left\{\left\langle b_i^m, \left(\nabla_t^2 + k_0^2 n^2(r)\right) b_j^m\right\rangle\right\}, \qquad i = 1,2,\ldots,N, \quad j = 1,2,\ldots,N, \tag{B10}$$

$$\mathbf{c} = \{c_i\}, \qquad i = 1,2,\ldots,N. \tag{B11}$$

The components of the eigenvectors $\mathbf{c}$ are the expansion coefficients c_i in Equation (B5). The technique enables the determination of the propagation coefficients and field distributions both for single-mode and multimode fibers.

REFERENCES

1. Sammut, R. A., "Analysis of approximations for the mode dispersion in monomode fibres," *Electron. Lett.*, Vol. 15, No. 19, 590–591, 1979.
2. Sharma, A. and S. Banerjee, "Chromatic dispersion in single mode fibers with arbitrary index profiles: A simple method for exact numerical evaluation," *J. Lightwave Technol.*, Vol. 7, No. 12, 1919–1923, 1989.
3. Kim, J. and D. Y. Kim, "An efficient dispersion calculation method for axially symmetric optical fibers," *Fiber Integrated Opt.*, Vol. 21, No. 1, 13–29, 2002.
4. Li, Q. Y., "Propagation characteristics of single-mode optical fibers with arbitrary refractive-index profile: The finite quadratic element approach," *J. Lightwave Technol.*, Vol. 9, No. 1, 22–26, 1991.
5. Boucouvalas, A. C. and X. Qian, "Mode dispersion and delay characteristics of optical waveguides using equivalent TL circuits," *IEEE J. Quantum Electron.*, Vol. 41, No. 7, 951–957, 2005.
6. Lin, H. Y., R. B. Wu, and H. C. Chang, "An efficient algorithm for determining the dispersion characteristics of single-mode optical fibers," *J. Lightwave Technol.*, Vol. 10, No. 6, 705–711, 1992.
7. Hermann, W. and D. U. Wiechert, "Refractive-index of doped and undoped PCVD bulk silica," *Mater. Res. Bull.*, Vol. 24, No. 9, 1083–1097, 1989.

8. Sharma, E. K., A. Sharma, and I. C. Goyal, "Propagation characteristics of single-mode optical fibers with arbitrary index profiles: A simple numerical approach," *IEEE J. Quantum Electron.*, Vol. 18, No. 10, 1484–1489, 1982.
9. South, C. R., "Total dispersion in step-index monomode fibres," *Electron. Lett.*, Vol. 15, No. 13, 394–395, 1979.
10. Mussina, R., B. P. de Hon, R. W. Smink, and A. G. Tijhuis, "Modal modeling strategies for the design of optical fibers," *Proceedings of Annual Symposium of IEEE/LEOS Benelux Chapter*, 199–202, University of Twente, The Netherlands, November, 27–28, 2008.
11. Mussina, R., D. R. Selviah, F. A. Fernández, A. G. Tijhuis, and B. P. de Hon, "Numerical modeling method for the dispersion characteristics of single-mode and multimode weakly-guiding optical fibers with arbitrary radial refractive index profiles," *Proc. SPIE* 8619, Physics and Simulation of Optoelectronic Devices XXI, 86191R, March 14, 2013; doi:10.1117/12.2002804; http://dx.doi.org/10.1117/12.2002804.
12. Thyagarajan, K., R. K. Varshney, P. Palai, A. K. Ghatak, and I. C. Goyal, "A novel design of a dispersion compensating fiber," *IEEE Photon. Technol. Lett.*, Vol. 8, No. 11, 1510–1512, 1996.
13. Thyagarajan, K. and B. P. Pal, "Modeling dispersion in optical fibers: Applications to dispersion tailoring and dispersion compensation," *J. Opt. Fiber Commun. Rep.*, Vol. 4, No. 3, 173–213, 2007.
14. Cohen, L. G. and W. L. Mammel, "Low-loss quadruple-clad single-mode lightguides with dispersion below 2 ps/km nm over the 1.28 µm–1.65 µm wavelength range," *Electron. Lett.*, Vol. 18, No. 24, 1023–1024, 1982.
15. Cohen, L. G., W. L. Mammel, and S. Limush, "Tailoring the shapes of dispersion spectra to control bandwidths in single-mode fibers," *Opt. Lett.*, Vol. 7, No. 4, 183–185, 1982.
16. Etzkorn, H. and W. E. Heinlein, "Low-dispersion single-mode silica fibre with undoped core and three F-doped claddings," *Electron. Lett.*, Vol. 20, No. 10, 423–424, 1984.
17. Smink, R. W., B. P. de Hon, M. Bingle, R. Mussina, and A. G. Tijhuis, "Refractive index profile optimisation for the design of optical fibres," *Opt. Quant. Electron.*, Vol. 40, No. 11–12, SPEC. ISS, 837–852, 2008.
18. Correia, D., V. F. Rodriguez-Esquerre, and H. E. Hernandez-Figueroa, "Genetic-algorithm and finite-element approach to the synthesis of dispersion-flattened fiber," *Microw. Opt. Technol. Lett.*, Vol. 31, No. 4, 245–248, 2001.
19. Wu, M. S., M. S. Lee, and W. H. Tsai, "Variational analysis of single-mode graded-core W-fibers," *J. Lightwave Technol.*, Vol. 14, No. 1, 121, 1996.
20. Zhang, X. P. and X. Wang, "The study of chromatic dispersion and chromatic dispersion slope of WI- and WII-type triple-clad single-mode fibers," *Opt. Laser Technol.*, Vol. 37, No. 2, 167–172, 2005.
21. Shahoei, H., H. Ghafoori-Fard, and A. Rostami, "A novel design methodology of multi-clad single mode optical fiber for broadband optical networks," *Progress In Electromagnetics Research*, Vol. 80, 253–275, 2008.
22. Rostami, A. and S. Makouei, "Modified W-type single-mode optical fiber design with ultra-low, flattened chromatic dispersion and ultra-high effective area for high bit rate long haul communications," *Progress In Electromagnetics Research C*, Vol. 12, 79–92, 2010.
23. Hooda, B. and V. Rastogi, "Segmented-core single mode optical fiber with ultra-large-effective-area, low dispersion slope and flattened dispersion for DWDM optical communication systems," *Progress In Electromagnetics Research B*, Vol. 51, 157–175, 2013.
24. Sharma, A. and J. P. Meunier, "On the scalar modal analysis of optical waveguides using approximate methods," *Opt. Commun.*, Vol. 281, No. 4, 592–599, 2008.
25. Meunier, J. P., J. Pigeon, and J. N. Massot, "A general approach to the numerical determination of modal propagation constants and field distributions of optical fibres," *Opt. Quant. Electron.*, Vol. 13, No. 1, 71–83, 1981.
26. Georg, O., "Use of the orthogonal system of Laguerre-Gaussian functions in the theory of circularly symmetric optical waveguides," *Appl. Optics*, Vol. 21, No. 1, 141–146, 1982.

27. Okamoto, K. and T. Okoshi, "Analysis of wave propagation in optical fibers having core with alpha-power refractive-index distribution and uniform cladding," *IEEE Trans. on Microw. and Theory*, Vol. 24, No. 7, 416–421, 1976.
28. Meunier, J. P., J. Pigeon, and J. N. Massot, "A numerical technique for the determination of propagation characteristics of inhomogeneous planar optical waveguides," *Opt. Quant. Electron.*, Vol. 15, 77–85, 1983.
29. Weisshaar, A., J. Li, R. L. Gallawa, and I. C. Goyal, "Vector and quasi-vector solutions for optical waveguide modes using efficient Galerkin's method with Hermite-Gauss basis functions," *J. Lightwave Technol.*, Vol. 13, No. 8, 1795–1800, 1995.
30. Wang, Z. H., H. Zhang, and J. P. Meunier, "Improved Ritz-Galerkin method for field distribution of graded-index optical fibers," *Microw. Opt. Technol. Lett.*, Vol. 37, 433–436, 2003.
31. Gallawa, R. L., I. C. Goyal, Y. Tu, and A. K. Ghatak, "Optical waveguide modes: An approximate solution using Galerkin's method with Hermite-Gauss basis functions," *IEEE J. Quantum Electron.*, Vol. 27, No. 3, 518–522, 1991.
32. Rasmussen, T., J. H. Povlsen, A. Bjarklev, O. Lumholt, B. Pedersen, and K. Rottwitt, "Detailed comparison of two approximate methods for the solution of the scalar wave-equation for a rectangular optical wave-guide," *J. Lightwave Technol.*, Vol. 11, No. 3, 429–433, 1993.
33. Barai, S. and A. Sharma, "Wavelet-Galerkin solver for the analysis of optical waveguides," *J. Opt. Soc. Am. A*, Vol. 26, No. 4, 931–937, 2009.
34. Erteza, I. and J. W. Goodman, "A scalar variational analysis of rectangular dielectric waveguides using Hermite-Gaussian modal approximations," *J. Lightwave Technol.*, Vol. 13, No. 3, 493–506, 1995.
35. Meunier, J. P. and S. I. Hosain, "An accurate splice loss analysis for single-mode graded-index fibers with mismatched parameters," *J. Lightwave Technol.*, Vol. 10, No. 11, 1521–1526, 1992.
36. Silvestre, E., T. Pinheiro-Ortega, P. Andrés, J. J. Miret, and A. Ortigosa-Blanch, "Analytical evaluation of chromatic dispersion in photonic crystal fibers," *Opt. Lett.*, Vol. 30, No. 5, 453–455, 2005.
37. Snyder, A. W. and J. D. Love, *Optical Waveguide Theory*, Chapman and Hall, London, 1983.
38. Wu, B. S., Z. H. Xu, and Z. G. Li, "A note on computing eigenvector derivatives with distinct and repeated eigenvalues," *Commun. Numer. Meth. En.*, Vol. 23, No. 3, 241–251, 2007.
39. Cho, J., C. T. Sun, and R. B. Nelson, "Simplified calculation of eigenvector derivatives," *AIAA J.*, Vol. 14, No. 9, 1201–1205, 1976.
40. Fleming, J. W., "Material dispersion in lightguide glasses," *Electron. Lett.*, Vol. 14, No. 11, 326–328, 1978.
41. Abramowitz, M. and I. A. Stegun, *Handbook of Mathematical Functions with Formulas*, Graphs, and Mathematical Tables, 9th Printing, Dover, New York, 1972.
42. Yamada, R., "Guided waves along an optical fiber with parabolic index profile," *J. Opt. Soc. Am.*, Vol. 67, No. 1, 96–103, 1977.
43. Fernández, F. A. and Y. Lu, *Microwave and Optical Waveguide Analysis by the Finite Element Method*, Wiley, New York, 1996.
44. Olshansky, R., "Propagation in glass optical waveguides," *Reviews of Modern Physics*, Vol. 51, No. 2, 341–367, 1979.
45. Senior, J. M., *Optical Fiber Communications: Principles and Practice*, 3rd Edition, Pearson Education Limited, 2009.
46. Gambling, W. A., H. Matsumura, and C. M. Ragdale, "Mode dispersion, material dispersion and profile dispersion in graded-index single-mode fibres," *IEE Proc. — H*, Vol. 3, No. 6, 239–246, 1979.